29th Congress of the International Council of the Aeronautical Sciences
St. Petersburg, Russia; September 7-12, 2014

INVESTIGATION OF THE TIP CLEARANCE EFFECT IN A COUNTER-ROTATING DUCTED FAN FOR VTOL UAV

Minhyoung Ryu*, Leesang Cho, Jinsoo Cho*****
***Department of Mechanical Engineering, Hanyang University, Seoul, Korea**
****Department of Mechanical Systems Engineering, Hansung University, Seoul, Korea**
*****School of Mechanical Engineering, Hanyang University, Seoul, Korea**

Keywords: *Ducted Fan, CFD, Aerodynamic analysis, Tip clearance, Duct, Wind tunnel*

Abstract

The tip clearance effect on counter-rotating ducted fan of VTOL UAV in hovering condition, was investigate using computational analysis. The numerical results of baseline model are validated by wind tunnel test in hovering and forward conditions. It is observed that if tip clearance of one rotor in the counter-rotating ducted fan increase then the thrust coefficient of another rotor increases. In Addition to this, when the tip clearance of the rear rotor increases, the thrust of the ducted fan is improved due to increasing of average total pressure at exit plane.

1 Introduction

UAVs (Unmanned Aerial Vehicle) are developing in most nations of the world. The UAV includes an aircraft, a controller on the ground and telecommunication equipment[1]. The existing UAV such as fixed and rotor blades have some demerits, for instance, they couldn't take-off and land vertically, they are dangerous to use in the town. In recent years, continuous monitoring through a vertical take-off and landing, and stop flying rotary-wing unmanned aerial vehicle was developed. Rotary-wing unmanned aircraft is somewhat difficult for individuals or small units used in the development of a small unmanned aircraft, using a ducted fan propulsion unit to personal mobile attempts have been made[2].

Ducted fan UAV can be used in the Future Combat System, a personal portable unmanned aircraft as compared to fixed-wing and rotary-wing unmanned aircraft is relatively small. In addition, the attitude is controlled by thrust ducted fan unmanned aircraft high propulsive efficiency compared to the existing rotary-wing unmanned aircraft. The rotational torque which is occurred from rotor can be reduced by stator. This outstanding machine has moving flap for thrust vector control.[3]

Akturk, etc. [4], the vertical / forward flight of short-range ducted fan unmanned aircraft for take-off and landing when the quiescent state and draughty in the state Computational Fluid Dynamics (CFD) Computational Fluid instrumentation analysis and particle image velocity (Particle Image Velocimetry affected by flow separation from the leading edge of the duct, PIV) measurement of flow through the drafts in forward flight conditions at the entrance of the ducted fan, and analyzed the impact on the ducted fan exit flow field. Entrance to the deformation of the flow field due to flow separation due to the shape of the duct shear force was decreased. Fleming et al. [5] the existing model and the auxiliary steering system installed for side winds and wind tunnel test model / stop when the flight battery was performed. Painted fan unmanned aircraft pitching moment with the use of the auxiliary steering system has been improved thanks to a 50% increased mobility.

Therefore, the aerodynamic characteristics of ducted fan are important for control. In this study, flow characteristics such as thrust coefficient, power coefficient and efficiency for various tip clearance were analyzed. The commercial software Ansys-CFX was used.

2 Wind tunnel test

2.1 Experimental setup

In order to verify the results of CFD analysis for counter-rotating ducted fan model, a wind tunnel test is performed.

Fig. 1. shows the subsonic wind tunnel in Hanyang university. The hovering, forward flight conditions of the counter-rotating ducted fan are tested. The test section is 800×800×1,200mm. The maximum velocity is 60m/s. The turbulence intensity is less than 0.2%. The blockage ratio is less than 1.1%. The aerodynamic characteristics are measured by 6-components load cell of CAS co, ltd. The capacity is 5kg. The resolution is 0.5%.

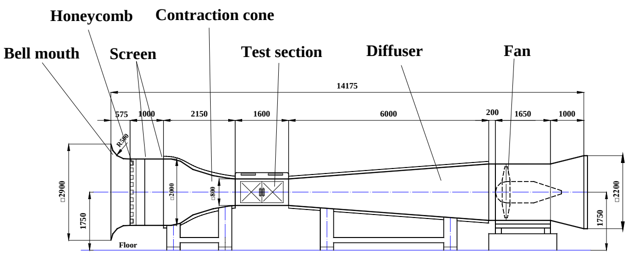

Fig. 1. Wind tunnel specification

2.2 Counter-rotating ducted fan model

Detailed specifications of the counter-rotating ducted fan are shown in table 1. The fan diameter is 150mm. The NACA 65 series airfoil is used in this study.

To evaluate an aerodynamic characteristics of the counter-rotating ducted fan, the performance variables are defined as follows:

$$\text{Advance ratio,}\ J = \frac{V_\infty}{nD} \tag{1}$$

$$\text{Thrust coefficient,}\ C_T = \frac{Thrust}{\rho n^2 D^4} \tag{2}$$

$$\text{Power coefficient,}\ C_P = \frac{Power}{\rho n^2 D^4} \tag{3}$$

$$\text{Efficiency,}\ \eta = J\frac{C_T}{C_P} \tag{4}$$

$$\text{Figure of merit,}\ FM = \frac{C_T^{1.5}}{\sqrt{2C_P}} \tag{5}$$

Figure. 2. is counter-rotating ducted fan model in the wind tunnel. The reynolds number of this model is 2.49×10^6. The mach number is 0.23. The tip clearance(t) is divided by radius(R) of ducted fan. The non-dimensional tip clearance ratio(t/R) of baseline model is 1.33%.

Table 1. Specifications for the baseline of the ducted fan

Parameter		Front rotor	Rear rotor
Fan diameter		150 mm	
Tip diameter		148 mm	
Hub diameter		37 mm	
Airfoil		NACA 65 series	
Chord length	hub	39.3 mm	42.7 mm
	mid	35.8 mm	35.1 mm
	tip	34.0 mm	34.0 mm
Stagger angle	hub	-41.7 deg.	54.9 deg.
	mid	-66.6 deg.	68.6 deg.
	tip	-73.6 deg.	74.1 deg.
Number of blades		3	
Rotational speed		10,000 rpm	-10,000 rpm

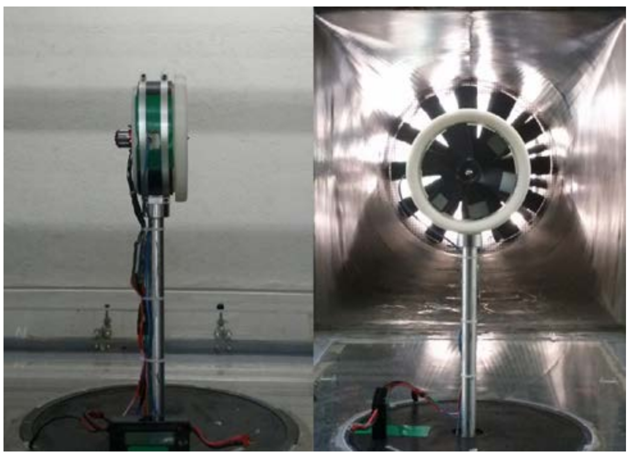

(a) Side view (b) Front view

Fig. 2. Test section of wind tunnel for the counter-rotating ducted fan

3 CFD analysis

3.1 Analysis model and boundary conditions

In order to evaluate the effect of the counter-rotating ducted fan is analyzed using Ansys CFX. The tip clearance ratio(t/R) of front and rear rotor is 0.67~5.33%. All models are calculated at hovering condition.

The CFX solver calculated Reynolds-Average Navier-Stokes(RANS) equations, which is based on finite volume method. The k-w SST turbulence model is used in this study. Fig. 3. shows computational domain and boundary condition of the analyzed model. The computational domain is consists of front, rear rotor, and outer region. The Multiple Frames of Reference(MFR) analysis model is used to connect rotating surface and stationary wall. The rotational speed of front and rear rotor is fixed to 10,000 RPM.

The boundary condition of inlet for outer domain was set to total pressure condition at hovering and velocity inlet at forward flight condition. The outlet boundary condition was set to pressure outlet (P_{gage}=0).The boundary conditions of front, rear rotor, hub and duct are determined to no-slip boundary conditions. The outer surface define opening boundary condition for hovering and free-slip wall for forward flight. In order to reduce computing time, the outer domain, front and rear rotor region were divided by 120° using periodic boundary conditions.

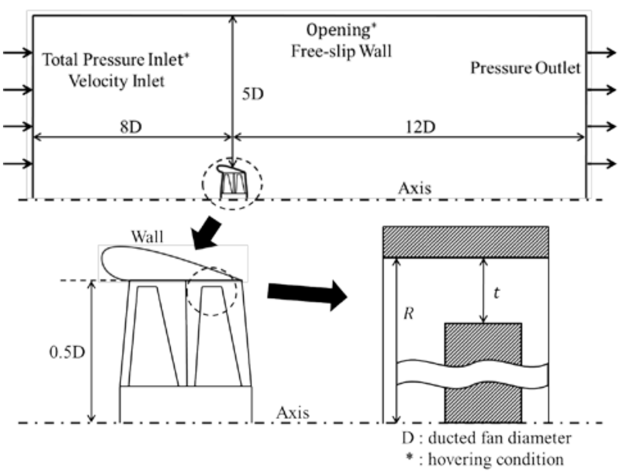

Fig. 3 Computational domain and the boundary conditions for the ducted fan.

3.2 Grid independent study

The outer domain has hexahedral grid, which is generated using ICEM CFD, as shown in Fig. 4. The grid of the front and rear rotor domain is generated by TurboGrid. All grids are composed of hexahedral mesh.

Figure. 5. shows results of grid independent study. The number of element is converged at 2.0×10^6. The computational grids have 2.0×10^6 elements. The number of elements for the rotating region is 8.6×10^5. The number of elements is 1.8×10^6 at outer region. For boundary layer analysis on the surface, the first layer thickness dimensionless wall distance is $y^+ \approx 1$, expansion ratio of 1.2 prism layer 30 layer is generated.

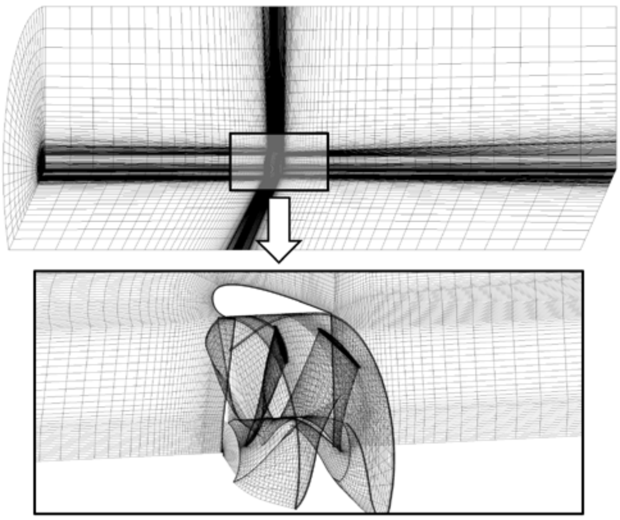

Fig. 4 Computation mesh for the ducted fan

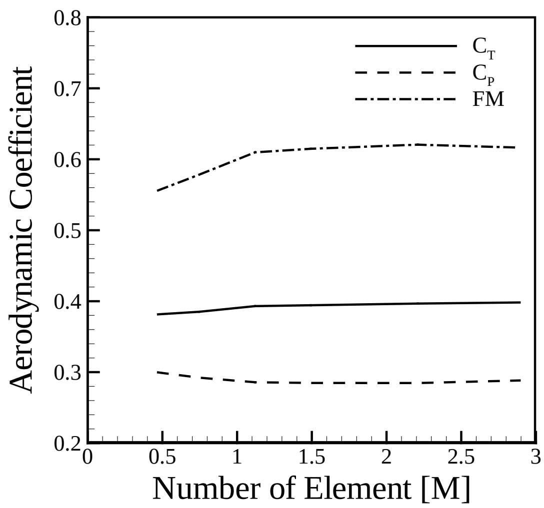

Fig. 5 Characteristic curves for the number of element

4 Results

4.1 Wind tunnel test

The wind tunnel test is performed for a validation of computational results. Fig. 6. shows experimental and computational results about thrust, power coefficient and efficiency of ducted fan. The computational results are good agreements with experimental results. The difference is less than 10%. The reason of error is the effect of model support.

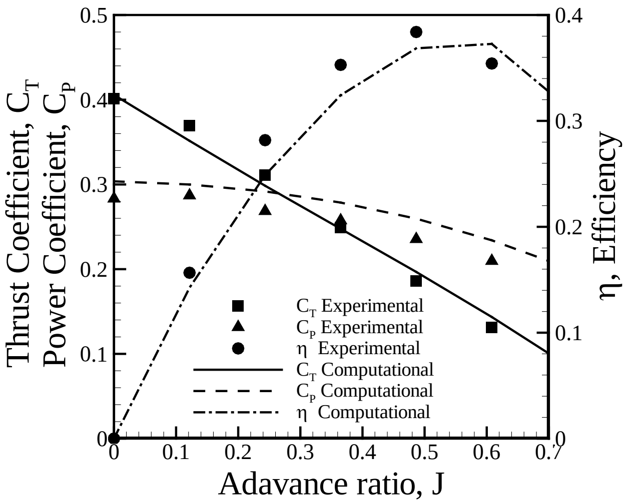

Fig. 6. Characteristic coefficient comparison of experimental and computational analysis for baseline

4.1 Aerodynamic characteristics for tip clearance

Figure. 7., 8. show the aerodynamic characteristics of the counter-rotating ducted fan to investigate the effect of tip clearance. The tip clearance(t/R) of rear rotor is fixed to 0.67, 1.33, 2.67, 4.00, 5.33% and vise versa. The tip clearance(t/R) of front rotor is set to 0.67~5.33%. The Figure of merit and thrust coefficient increases along with increase of the tip clearance of front rotor. The power coefficient is decreased at $(t/R)_{Rear}$=2.67, 4.00, 5.33%.The maximum figure of merit occured at (t/R)Front=0.67%, (t/R)Rear=0.67%. The figure of merit is higher 3.45% than baseline model. And the maximum thrust is confirmed at (t/R)Front=0.67%, (t/R)Rear=5.67%.

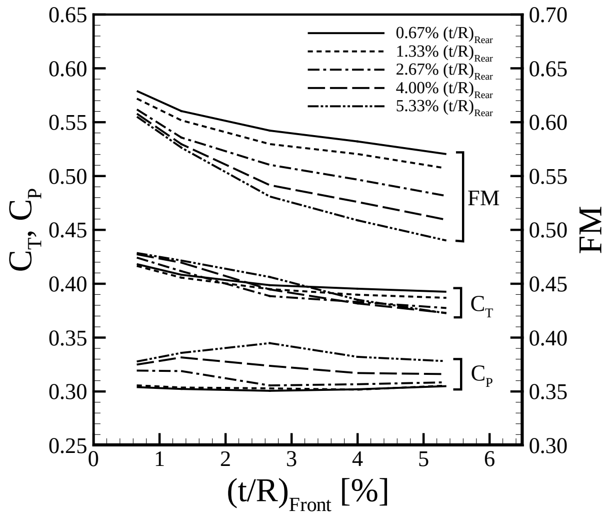

Fig. 7. Characteristic curves versus tip clearance of the rear rotor for a hovering ducted fan

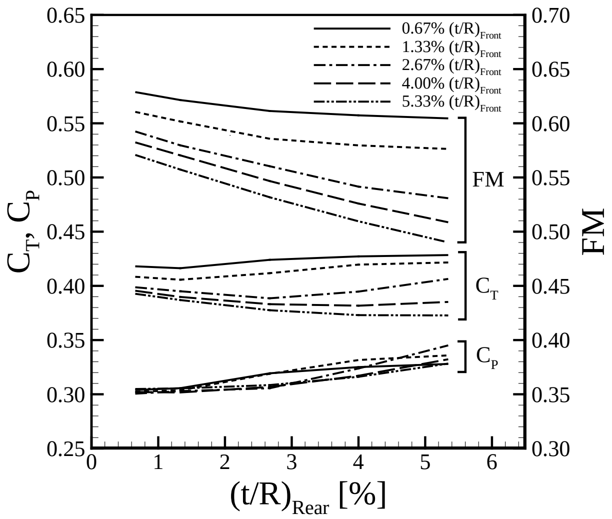

Fig. 8. Characteristic curves versus tip clearance of the rear rotor for a hovering ducted fan

4.2 Flow filed analysis

Figure. 9. shows a axial velocity contour of counter-rotating ducted fan. The left figure is $(t/R)_{Rear}$ = 1.33%. And the right side means $(t/R)_{Rear}$ = 4.00%. The axial velocity component is divided by blade tip speed(U_{tip}) for non-dimension. The region of tip leakage flow is narrowed at rear rotor due to increase of tip clearance of rear rotor.

If the tip clearance of the rear rotor is larger than the front rotor, the thrust increases. Because the region of tip leakage flow decreased. The averaged velocity components are increased at exit of ducted fan. The thrust is increased.

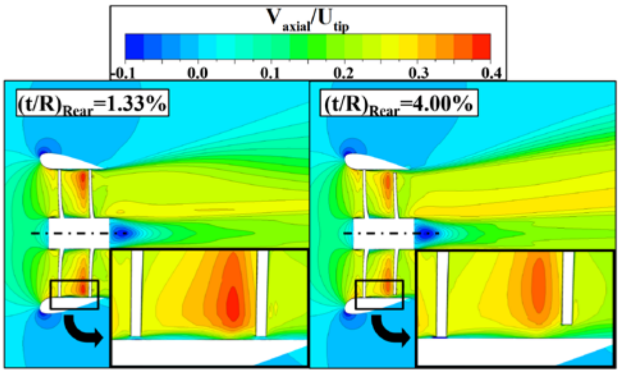

Fig. 9. Axial velocity distribution comparison for ducted fan with rear rotor of 1.33% and 4.00% tip clearance

5 Conclusion

In this study, CFD analysis and wind tunnel test of the counter-rotating ducted fan were performed on the hovering and forward flight conditions. The numerical results are good agreement with experimental results.

If the tip clearance of some rotor, the thrust is increased at the counter-rotating ducted fan. The effect of the tip clearance of the rear rotor is large portion of total thrust in the counter-rotating ducted fan. The thrust coefficient is increased as a large tip clearance of the rear rotor.

To find an optimal tip clearance of each rotor in the counter-rotating ducted fan, the optimal design process is need in the future.

Acknowledgments

This research was supported by Basic Science Research Program through the National Research Foundation of Korea(NRF) funded by the Ministry of Education(No. 2009-009072).

References

[1] F. Marc de Piolenc, George E. Wright Jr., *Ducted Fan Design*, Mass Flow, Vol. 1, 2002.

[2] Akturk, A., Shavalikul, A., and Camci, C., "PIV Measurements and Computational Study of a 5-Inch Ducted Fan for V/STOL UAV Applications," *47th AIAA Aerospace Sciences Meeting and Exhibit*, Orlando, Florida, 2009, pp. 5-8.

[3] Akturk, A., and Camci, C., "Tip Clearance Investigation of a Ducted Fan used in VTOL UAVs, Part 1: Baseline Experiments and Computational Validation," *Proceedings of the ASME Turbo Expo Turbine Technical Conference*, 2011.

[4] Cho, J., Won, Y., Lee, M., "Numerical and Experimental Analyses of the Aerodynamic Characteristics of a Counter Rotating Axial Fan,“ *Transactions of the Korean Society of mechanical engineers-B*, Vol. 24, No. 3, 2000, pp. 325-337.

[5] Ko, K., Jung, H., Kim, D., and Cho, J., "Study on the Aerodynamic Characteristics of Hanyang Low Speed Wind Tunnel," *Journal of The Korean Society for Aeronautical and Space Sciences*, Vol. 31, No. 4, 2003, pp. 92-98.

[6] Leishman, J. Gordon, Principles of *Helicopter Aerodynamics*, Cambridge University Press, 2000.

[7] Menter, F. R., "Two-equation eddy-viscosity turbulence models for engineering applications," *AIAA journal*, Vol. 32, No. 8, 1994.

[8] Bardina, J., Huang, P., and Coakley, T., "Turbulence modeling validation, testing, and development," Technical Report, NASA Technical Memorandum 110446, 1997.

[9] ANSYS, Inc., ANSYS CFX-Solver Theory Guide, Release 13.0, 2010.